Available online at www.sciencedirect.com
SCIENCE DIRECT®
Journal of Luminescence 115 (2005) 138–146
JOURNAL OF LUMINESCENCE
www.elsevier.com/locate/jlumin

Photoinduced electron transfer in the head group region of sodium dodecyl sulfate micelles

J. Nanda*, P.K. Behera[1], H.L. Tavernier[2], M.D. Fayer

Department of Chemistry, Stanford University, Stanford, California 94305, USA

Received 28 August 2004
Available online 21 April 2005

Abstract

Photoinduced electron transfer between octadecylrhodamine B (a hole donor) and *N*, *N*-dimethyl-1-napthylamine (hole acceptor), located in the head group region of sodium dodecylsulfonate micelles, has been examined for different acceptor concentrations using time resolved fluorescence. The experimental results were analyzed using the Marcus distance-dependent transfer rate modified to take into account the heterogeneous nature of the micelles. Diffusion of the donor/acceptors is included in the theoretical analysis. The results are compared with earlier experiments involving the same donor–acceptor combination but in a different type of micelle.

PACS: 78.47.+p; 82.33.Nq; 82.70.Uv

Keywords: Electron transfer; Time resolved fluorescence, Micelles

1. Introduction

Electron transfer in condensed phases has been under intensive investigation for over 50 years [1–3]. Quantitative understanding of the electron transfer processes in a range of media can provide direction for designing efficient light harvesting systems involving chemical and biological complexes [4–6]. However, the intricacy of the electron transfer process in topologically complex systems in which donors and acceptors are changing their relative positions makes the quantitative description of such systems difficult. The time dependence of electron transfer depends on the electronic properties of the donors and acceptors, as well as the structure and morphology of the local environment [7–10]. Typically, intermolecular electron

*Corresponding author. Present address: Los-Alamos National Laboratory, Chemistry Division, MS-J585, C-PCS, Los Alamos, NM 87545, USA. Tel.: +1 505 665 3526; fax: +1 505 667 7289.
E-mail address: nanda@lanl.gov (J. Nanda).
[1]Permanent address: Department of Chemistry, Sambalpur University, Sambalpur 768 019, India.
[2]Present address: Department of Chemistry, Wellesley College, Wellesley, MA 02481, USA

0022-2313/$ - see front matter © 2005 Elsevier B.V. All rights reserved.
doi:10.1016/j.jlumin.2005.03.007

transfer occurs on a distance scale of a few Angstroms, making the process sensitive to the details of the local environmental [11,12]. Systems like micelles, reverse micelles, and vesicles are media with spatially restricted geometries and dielectric heterogeneity [13–16].

Here, we present time-resolved fluorescence and fluorescence yield data for photoinduced electron transfer from *N*, *N*-dimethyl-1-napthylamine (DMNA) to octadecylrhodamine B (ODRB), which are located in the head group region of micelles composed of the anionic surfactant, sodium dodecylsulfonate (SDS). The ODRB is low in concentration and is optically excited. For these reasons, ODRB will be called the donor; it is a hole donor. DMNA is the hole acceptor. Various concentrations of DMNA acceptors are employed. The ODRB is anchored in the micelle by its long hydrocarbon tail with the RB chromophore located in the head group region because of its positive charge. The polarity of the DMNA also causes it to locate almost exclusively in the head group region [17]. Therefore, the dynamics of the electron transfer can be modeled as a donor interacting with a number of acceptors all of which are constrained to move in the essentially spherical head group region.

A previous study investigated this problem for micelles that had cationic head groups of trimethylamines [17]. In the previous study the head groups were positively charged. In this study, the head groups are negatively charged. The ODRB donor is positively charged. In the analysis that was applied previously and is used again here, no specific account was taken of the role of the changes on the head groups and the ODRB may play. The detailed analysis took into account the spherical topology of micelles, the confinement of the donors and acceptors to the head group region, and the inhomogeneous nature of the system. Because the donor and acceptor used here are the same as those studied previously, changing the charge on the head groups enables us to determine if the nature of the head groups plays a fundamental role in the electron transfer process or if the key is the size and topology of the system with the change of on the head group having little or no effect.

The experimental results are analyzed using a statistical mechanical theory that describes the electron transfer for donors and acceptors diffusing in a spherical shell. Unlike donors and acceptors in a liquid, which can be approximated as a single dielectric continuum, the dielectric environment of the donors and acceptors in the head group region of micelles is heterogeneous. The head group region has dielectric properties that are intermediate between the very low dielectric constant hydrocarbon core and the very high dielectric constant surrounding water. Thus, the donor and acceptor confined in the head group region of the micelles experience a complex dielectric environment compared to a single dielectric continuum. The reorganization energy and free energy that play a role in electron transfer are modified by the micelle's multilayer structure [7]. The complex dielectric structure of the micelles is included in the theoretical analysis of the data [17]. The results are compared with the electron transfer parameters obtained from previous experiments involving the same donor/acceptor but different micelles [17].

2. Experimental procedures

ODRB was obtained from Molecular Probes and was used without purification. DMNA and SDS were obtained from Aldrich in highest grade available. The surfactant, SDS, concentration [*S*], was 2.046×10^{-2} M which corresponds to a micelle concentration [*M*], of 206 μM as determined using the relation

$$[M] = \frac{[S] - \mathrm{cmc}}{N_{\mathrm{agg}}}, \tag{1}$$

where cmc denotes the critical micelle concentration, and N_{agg} is the aggregation number. For SDS micelles, the cmc is 8.1 mM and the aggregation number is 60 [18]. The ODRB concentration was kept at 20 μM, a factor of about 10 less than that of the micelles. This ensures that there is at the most one ODRB per micelle. The chemical structure of ODRB, DMNA, and SDS are given in Fig. 1.

Four samples were prepared: one sample was made with only ODRB, and three samples were

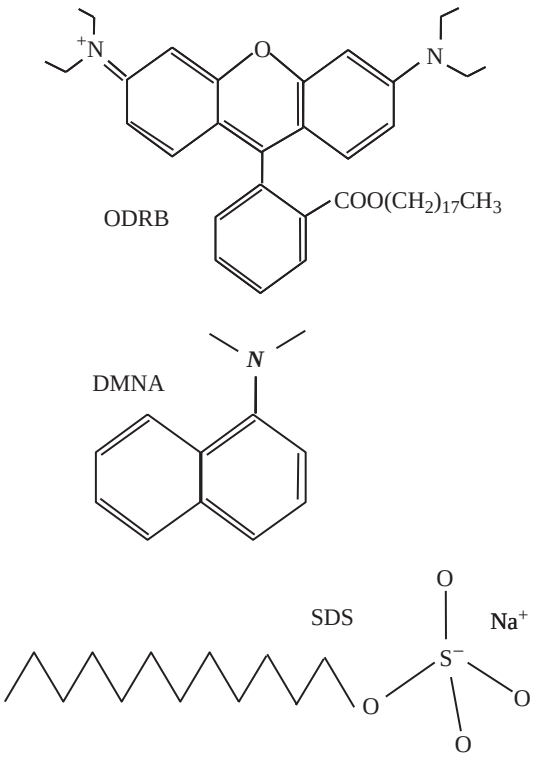

Fig. 1. Chemical structure of ODRB, DMNA and SDS.

made with ODRB with three different DMNA concentrations. In all of the samples, the ODRB concentration was kept the same with only the acceptor (DMNA) concentration varying. DMNA shows close to 100% binding to DTAB, TTAB, and CTAB micelles (TAB = trimethylammonium bromide; D = dodecyl; T = tetradecyl; C = hexadecyl) [17] and the same was assumed to be the case for SDS micelles. DMA has been shown to reside in the head group region of CTAB micelles by NMR chemical shift measurements [19]. Confirmation of the location of DMNA in XTAB micelles was obtained from fluorescence spectroscopy [17]. We also expect DMNA to be located in the head group region of the SDS micelles because of the polarity considerations.

The fluorescence decays were measured using time-correlated single photon counting [20]. A Rhodamine 6G dye laser (568 nm) was synchronously pumped by the 532 nm doubled cavity dumped output of a mode-locked Nd:YLF laser. The laser output repetition rate was 800 kHz and the pulse duration was 15 ps. The fluorescence was collected using a front surface geometry and then passed through a subtractive double monochromator set at 590 nm (corresponding to the fluorescence peak of ODRB) and detected with a channel plate detector. The instrument response function was about ~75 ps FWHM. The polarization of the excitation beam was set at the magic angle of 54.7° with respect to the polarizer in front of the monochromator. For quantum yield measurements, the steady-state florescence measurements for samples with various acceptor concentrations were corrected for ODRB concentration and compared to fluorescence from a sample without acceptors.

3. Theoretical formulation

Fig. 2a shows a schematic of the micelle. The hydrocarbon core is surrounded by the head group region, which is in turn surrounded by water. Counter ions and water penetrate into the head group region to some extent, giving it a dielectric constant that is intermediate between the hydrocarbon core (low dielectric constant) and the water (high dielectric constant). Fig. 2b shows the model used in the theoretical calculations. The donor is the black ball, and the acceptors are grey. The donors and acceptors are centered in the head group region. The distance, r, between the donor (D) and an acceptor (A) is determined by the distance R and the angle, γ. R is the average of a_c (core radius) and a_s (core radius plus the head group shell radius). The distance between the donor and an acceptor is

$$r = 2R \sin(\gamma/2). \quad (2)$$

The contact distance is $r_m = 2R \sin(\gamma_m/2)$. The radii of D and A are a_D and a_A, respectively. The donor and acceptors are diffusing in the head group spherical shell.

An analytical theory, evaluated numerically, for calculating the electron transfer dynamics between a donor and acceptors in the head group regions of micelles has been presented [7,17,21–24]. Here, we provide a brief account of the essential features of

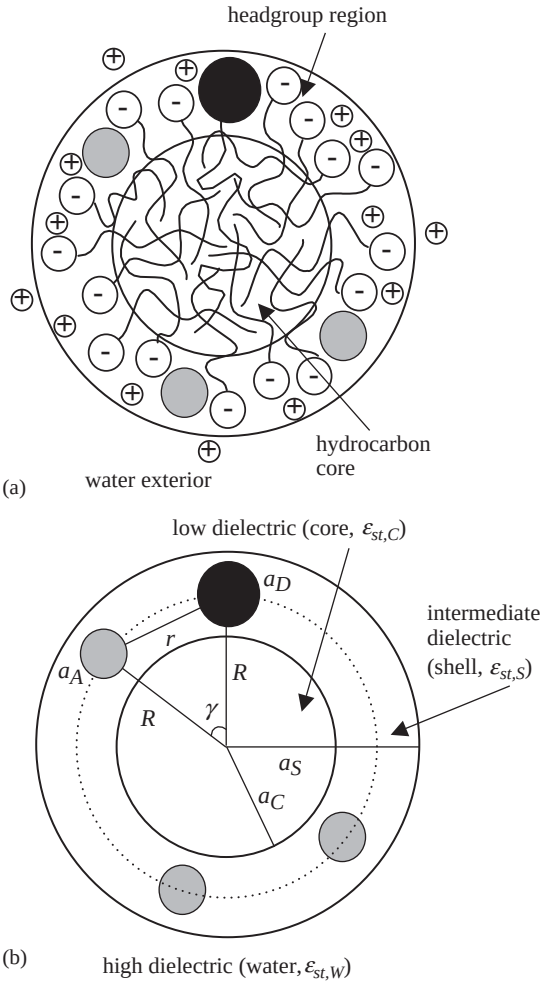

Fig. 2. (a) Schematic diagram of a micelle, indicating three regions. The region inside the smaller circle contains the surfactant tails and is the hydrocarbon core. The region outside the largest circle is water with counter ions. The shell between the two circles is the region of surfactant head groups (−), most of the counter ions (+), the (hole) donor (black) and (hole) acceptor molecules (shaded), and portions of the surfactants' hydrocarbon tails. The dielectric properties of head group region are intermediate between those of water and hydrocarbon. (b) Model for electron transfer in the head group region of a micelle, incorporating 3-region dielectric structure. The donor and acceptor spheres, with radii $a_{D/A}$, lie at distances $R_{D/A}$ from the center of the micelle and diffuse on spherical surfaces with radius R. r is the distance between the donor and an acceptor. γ is the angle between the lines joining the center of the micelle with the centers of a donor and an acceptor pair. The interior of the micelle is taken to be a sphere of radius a_C with a low static dielectric constant. Donor and acceptor spheres are located outside the micelle core in a shell of radius a_S that surrounds the micelle core. Finally, the shell is surrounded by water.

the theory required to analyze the data. Following photoexcitation of the single donor per micelle, the system either relaxes to the ground state or an electron is transferred. If an electron is transferred, the system is in the "charge transfer state" and fluorescence does not occur. The free energy change, $\Delta G(r)$ associated with photoinduced electron transfer is given by a general expression:

$$\Delta G(r) = \mathrm{IP_D} - \mathrm{EA_A} - W_\mathrm{r} + W_\mathrm{p} - h\nu, \tag{3}$$

where $\mathrm{IP_D}$ is the ionization potential of the donor, $\mathrm{EA_A}$ is the electron affinity of the acceptor, $W_{r/p}$ denote the total energy change to bring the reactants/products together in the dielectric environment of interest at the given separation distance, and $h\nu$ is the donor singlet excited state energy, taken to be the energy at which donor's normalized absorption and fluorescence spectra cross [25]. For a heterogeneous system like the micelles the distances dependent free energy change $\Delta G(r)$ was calculated from the redox potential measured for the bulk solution as described in detail previously [17].

The experimental observable is $\langle P_\mathrm{ex}(t)\rangle$, the probability that a donor excited at $t = 0$ is still excited at time, t. $\langle P_\mathrm{ex}(t)\rangle$ is proportional to the fluorescence intensity. Assuming the number of acceptor molecules in the micelles have a Poisson distribution about the mean number of acceptors N, the observable is

$$\langle P_\mathrm{ex}(t)\rangle = \sum_{n=0}^{\infty} \frac{\mathrm{e}^{-N} N^n}{n!} \langle P_\mathrm{ex}(t)\rangle_n, \tag{4}$$

where $\langle P_\mathrm{ex}(t)\rangle_n$ describes a micelle with one donor and exactly n acceptors.

$$\langle P_\mathrm{ex}(t)\rangle_n = \mathrm{e}^{-t/\tau}\left[\int_{\gamma_m}^{\pi} S_\mathrm{ex}(t|\gamma_0) 2\pi R^2 \sin\gamma_0 g(\gamma_0)\,\mathrm{d}\gamma_0\right]^n, \tag{5}$$

where τ is the fluorescence lifetime of the donor in the absence of the acceptor. $S_\mathrm{ex}(t|\gamma_0)$ is the probability that the donor is still excited at time t, given that it was photoexcited at $t = 0$ and that the donor and acceptor were separated by angle γ_0 (distance r) at that time, for the one-donor, one-acceptor case [21,22]. $S_\mathrm{ex}(t|\gamma_0)$ is the solution to a differential equation, which has been described in detail previously [17,21,22]. $g(\gamma)$ is the radial

distribution function used to model the donor–acceptor distance distribution in the head group region [17]. $S_{ex}(t|\gamma_0)$ depends on the distance dependence of the transfer rate as well as the dielectric properties of the micelle.

The Marcus form of the distance-dependent transfer is employed (normal region, $\Delta G < \lambda$) [1,2,26].

$$k(r) = \frac{2\pi}{\hbar} J_0^2 \exp[-\beta(r - r_m)] \times \frac{1}{\sqrt{4\pi\lambda k_B T}} \exp\left[\frac{-(\Delta G(r) + \lambda(r))^2}{4\lambda k_B T}\right]. \quad (6)$$

$\hbar$ is the Planck's constant, k_B is the Boltzmann's constant, and T is the temperature. J_0 is the donor–acceptor electronic coupling strength at contact, and β is the exponential decay constant for the electric coupling. $\Delta G(r)$ is the free energy change of the transfer and $\lambda(r)$ is the solvent reorganization energy. The standard expressions for $\Delta G(r)$ [27] and $\lambda(r)$ [1,2,26,28] are for donors and acceptors in a dielectric continuum. These are substantially modified for the heterogeneous dielectric environment associated with a donor and acceptors in the head group regions of micelles (see Fig. 2b). Expressions for $\Delta G(r)$ and $\lambda(r)$ for the head group region have been derived [7,17]. The important point here is that the expressions for $\Delta G(r)$ and $\lambda(r)$ depend on the dielectric constant of the core, the head group region, and the surrounding water. These expressions [7,17] are used in the calculations presented below. The polyelectrolyte nature of the micelle surface (charged head groups and counter ions) has not been included in the analysis. This, however, has been shown in other systems to have a minor effect compared to the polarity of the solvents [29].

The spatial distribution of the donor and acceptors comes into Eq. (4). A hard sphere $g(r)$ is used with the donor–acceptor contact distance as the minimum distance, r_m [17]. It has been shown for hard sphere liquids that a solute's spatial distribution follows the solvent's radial distribution function, $g(r)$ [30]. (Here, $g(r)$ becomes $g(\gamma)$ in the actual calculations.) The donor and acceptors are not in high enough concentration to independently form a structured distribution; under normal circumstances, it is assumed that they follow the structure determined by the solvent molecules [30]. The size, σ, used to describe the "solvent molecules" for the head group region of SDS will be discussed below. Diffusion is constrained by the fact that the equilibrium distribution of acceptor molecules must follow the solvent's radial distribution function, $g(r)$. As a result, molecular diffusion occurs within a potential of mean force ($-\ln[g(r)]$) rather than freely [31,32]. The effects are strongest within the first solvent shell. In addition, as the donor and acceptor approach each other, the effective diffusion constant is reduced [33,34]. The reduction of the diffusion constant on close approach is called the hydrodynamic effect [35,36], and it is included in the theory via a distance-dependent diffusion constant, $D(r)$ given by the expression [17,33,34]

$$D(r) = D\left[1 - \frac{1}{2}\exp\left(\frac{r_m - r}{\sigma}\right)\right], \quad (7)$$

where D is the sum of the donor and acceptor bulk diffusion coefficients, r_m is the donor–acceptor contact distance, and σ is the solvent diameter.

Donor–acceptor diffusion in the head group region will be dominated by the diffusion of the DMNA because the ODRB is anchored in the micelle by its long hydrocarbon tail. Detailed measurements have been made to determine the diffusion constant in XTAB micelles [17]. The value is $D = 15.9\,\text{Å}^2/\text{ns}$. This value is expected to be different in the case of SDS head groups as will be discussed later in the text.

Because of the time resolution of the instrument, ~75 ps, information about the short time behavior of electron transfer is masked. Some additional information can be obtained from the fluorescence yield measurements. The fluorescence yield, Φ is the ratio of the total steady-state fluorescence for a sample containing DMNA to that of a sample consisting only ODRB.

$$\Phi = \frac{\int_0^\infty \langle P_{ex}(t)\rangle \, dt}{\tau}. \quad (8)$$

Thus, fluorescence yield experiments are sensitive to integrated area of $\langle P_{ex}(t)\rangle$, which does not include convolution with the instrument response function.

4. Results and discussion

The steady state absorption spectra of the SDS/ODRB/DMNA corresponding to three different concentration of DMNA are shown in Fig. 3. The ground state absorption spectrum of ODRB has two distinct peaks at 559 and 521 nm as shown by the magnified spectrum in the inset. However, the DMNA absorption features are masked due to the strong absorption from SDS micelles at wavelengths below 300 nm. Our previous experiments on DMNA on different micellar system shows three distinct absorption features positioned at 298, 250 and 214 nm, respectively. The steady state fluorescence spectra of the samples for all acceptor concentrations show a fluorescence maximum at 590 nm (not shown here).

Fig. 4 shows the fluorescence decay curves of ODRB in SDS micelles for four concentrations of DMNA, 0.0, 4.8×10^{-4}, 7.9×10^{-4}, and 1.15×10^{-3} M, from top to bottom. These correspond to an average number of DMNA acceptors in a micelle of $N = 0$, 2.4, 3.96 and 5.78. There is at most one ODRB per micelle. For $N = 0$, the fluorescence decay curve is a single exponential with a decay time of 2.48 ns. Upon increasing the concentration of DMNA, the decays become faster as electron transfer from DMNA to ODRB

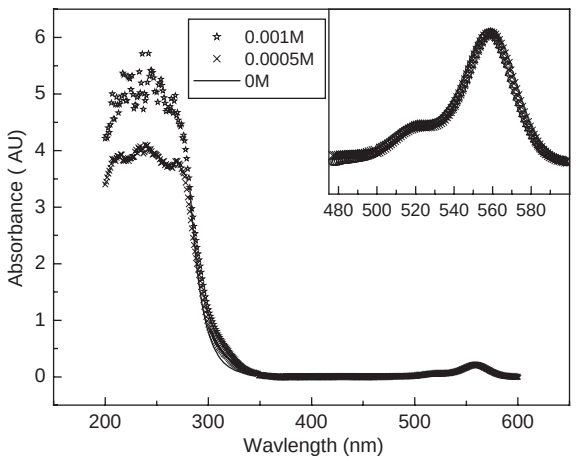

Fig. 3. Steady state optical absorption spectra of SDS/ODRB/DMNA with 0.001 M (star) and 0.0005 M (cross) DMNA, respectively. The solid line is the spectrum with no acceptors. The inset shows the magnified region of ODRB absorption.

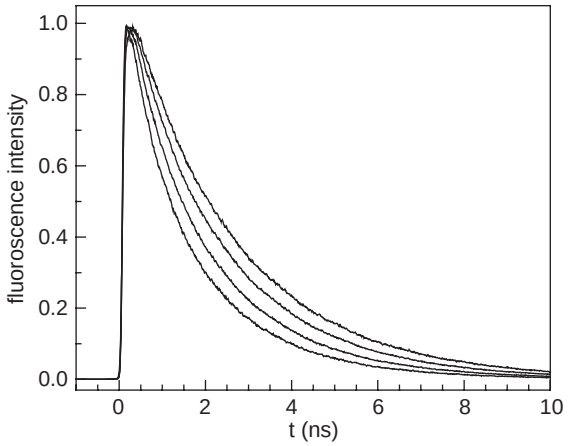

Fig. 4. Fluorescence decay curves of ODRB in SDS/water solvent with four DMNA concentrations. From top to bottom the average numbers of DMNA hole acceptors per micelle are: $N = 0$, 2.4, 3.96, and 5.78. As the acceptor concentration increases, the decays become fast because of the increased rate of electron transfer.

quenches the fluorescence at an increasing rate. The decays show clear deviations from being single exponential. In fact, fluorescence decay curves can be accurately fitted to a bi-exponential function showing two distinct time components τ_1 and τ_2 with respective amplitudes A_1 and A_2. The time constants derived from the fitting are τ_1=1.58 ($A_1 = 0.434$), 1.2($A_1 = 0.48$), 0.92($A_1 = 0.52$) ns and $\tau_2 = 2.5$ ($A_2 = 0.71$), 2.32($A_2 = 0.65$), 1.65($A_2 = 0.60$) ns, respectively, with increasing acceptor concentrations ($N = 2.4$, 3.96, and 5.78). However, the bi-exponential fit is only heuristic. The theoretical curves are continuous non-exponentials.

For each of the three DMNA concentrations the fluorescence decay and the fluorescence yield data were simultaneously fit. The value of β, the parameter that characterizes the distance dependence of the electronic coupling, is $\sim 1\,\text{Å}^{-1}$ in a variety of different electron transfer systems [2,37–40]. In the earlier experiments involving R3B and DMA in liquids the data fitted well with $\beta = 1\,\text{Å}^{-1}$. Therefore, to reduce the number of adjustable parameters β was fixed at a value of $1\,\text{Å}^{-1}$. Small angle X-ray scattering experiments carried out for SDS micelles in water by Itri and Amral and others measure a hydrocarbon core

radius of 16.7 Å and the overall size ranging between 22 and 23 Å [18,41]. The hard sphere radii of ODRB and DMNA were obtained from molecular modeling and are 4.12 and 3.09 Å, respectively, which gives a distance of closest approach of 7.21 Å. The optical and static dielectric constant for hexane, $\varepsilon_{op} = \varepsilon_{st} = 1.88$, were used for the micelle's hydrocarbon core. For water surrounding the micelles, $\varepsilon_{op} = 1.77$ and $\varepsilon_{st} = 78.3$. Optical dielectric constant of the head group region did not significantly affect the fits, so $\varepsilon_{op} = 1.9$ was used. The oxidation potential of DMNA in acetonitrile vs. SCE is 1.01 V and the difference in the redox potential in bulk solution between DMNA/ODRB was calculated to be 1.29 V.

The value of J_0 obtained from previous fitting results of DMNA/ODRB in CTAB was 70 cm^{-1} [17]. J_0 is the electronic coupling at contact. Therefore, it is reasonable to assume that this value is independent of the details of the micelle head groups, and we have used 70 cm^{-1} in the current analysis. With most of the input parameters for the calculation of $\langle P_{ex}(t)\rangle$ known or estimated, three remaining parameters were used to fit the concentration-dependent decay curves and the quantum yield measurements. They are: the head group properties, σ and $\varepsilon_{st,S}$ (the subscript S is for shell, see Fig. 2) and the diffusion constant, D. D was constrained to be similar to the value determined for the head group region of DTAB [17]. However, the size of the head group region is not the same in SDS and DTAB, and therefore, D was allowed to vary around the DTAB value.

The results of the fits are shown in Fig. 5 as the dashed lines through the data. $D = 28\,Å^2/ns$, which is comparable to the value of $16\,Å^2/ns$ determined for DMNA in DTAB micelles based on orientational relaxation measurements [17]. The values of σ and $\varepsilon_{st,S}$ returned good fits to the time-dependent data over a narrow range of values. $\sigma = 2-4$ Å and $\varepsilon_{st,S} = 8-16$. While the time-dependent data are fit very well by the model, the yield calculations do not agree as well with the yield data. A similar deviation, in which the calculated yields are too small but the time-dependent data fit very well was seen in

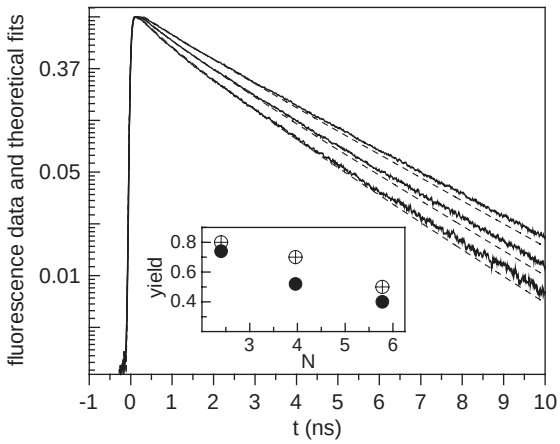

Fig. 5. Experimental fluorescence decay curves (solid) and $\langle P_{ex}(t)\rangle$ theoretical fits(dashed) for three concentrations of DMNA. From top to bottom the average numbers of DMNA hole acceptors per micelle are: $N = 2.4$, 3.96, and 5.78. The inset shows the experimental fluorescence quantum yields. The circles with crosses are the experimental data and the solid circles are calculated from the fits to the time-dependent data. While the fits to the time-dependent data are excellent, the yield calculations show significant deviation, which may indicate that the fits to the >100 ps data do not capture the short time electron transfer dynamics properly.

experiments with the same donor and acceptor in DTAB [17]. In the DTAB system, the agreement was better, but the trend was the same. The time-dependent data are for $t > 100$ ps. The fact that the calculated yield data are too small suggests that electron transfer at short time is slower than the current model predicts. Future experiments will examine electron transfer in micelles down to 100 fs, three orders of magnitude faster, to determine the nature of the transfer at very short times where both spatial and orientational diffusion play less of a role in the electron transfer kinetics.

A value of 10 for the dielectric constant of the head group region implies that it is relatively nonpolar compared to the surrounding region, water, which has a dielectric constant of 78, but it has a substantially higher dielectric constant than the micelle's hydrocarbon core. The head group region of a micelle contains both the actual head group and the first few methylenes that have some water penetration. In the experiments on XTAB micelles, values for CTAB, TTAB, and DTAB

were found to be 6, 30 and 30 [17]. Neutron scattering results show that there is considerably less water in the head group region of CTAB than in DTAB [42]. The value for SDS is closer to the CTAB value than the DTAB, which is more similar in size to SDS. A low value of the dielectric constant in the head group region suggests less water penetration.

The effect of $D(r)$ on the fitting was insignificant as the fits were basically the same using a distance independent diffusion constant. The value of σ (the "solvent size," that is hard sphere diameter) used in $g(r)$ gave good results in the range of 2–4 Å, with $\sigma = 3$ Å giving a slightly better result. This is close to the radius of the SDS head group. Hence the fact that a hard sphere solvent diameter of 3 Å is required to model the donor–acceptor distance distribution suggests that the SDS head groups rather than the much smaller water molecules that are present in the head group region play the dominant role in determining the spatial distribution of DMNA relative to ODRB. In the XTAB micelles, $\sigma = 5$ Å was used in the fits, which corresponds to the larger size of the head groups in these micelles. The theoretical fits for all three acceptor concentrations deviate from the experimental electron transfer data at longer time scales (>5 ns) as shown in Fig. 5. This could be due to slow solvation dynamics in the SDS micelles.

5. Concluding remarks

In this paper, electron transfer between ODRB and DMNA on the surface of SDS micelle for different acceptor (DMNA) concentrations was measured experimentally and analyzed theoretically. Time-dependent fluorescence and fluorescence yield data were measured for each concentration. These data were analyzed using the Marcus distance-dependent transfer rate using a model that takes into account the heterogeneous nature of the micelle structure. Although we have highly simplified the real structure of the micelles for modeling the experimental results theoretically, the model nevertheless includes all the important parameters that control the electron transfer in such a restricted geometry. While there are a large number of parameters that go into the fitting the data, most of them are either known or could be estimated with reasonable accuracy. It is important to note that the decay curves are non-exponential. The theory must reproduce the shapes of the decays and their concentration dependence. As in the previous study of the same donor and acceptor in XTAB micelles, it is found that on a time scale set by the time resolution of the instrument, >100 ps, the theory is very successful. However, the agreement between theory and calculations are worse for the quantum yield data, indicating that the dynamics at short times, substantially less than 100 ps, may not be described as well by the current model.

In comparing the experiments performed here in SDS micelles and the previous experiments in XTAB micelles, it is found that the same basic theory with similar parameters can do a good job of fitting the data in both types of micelles. The ODRB is positively charged. The SDS head groups are negatively charged while the XTAB head groups are positively charged. The fact that essentially the same description works reasonably well to describe electron transfer in both types of micelles suggests that specific Coulombic interactions between the ODRB hole donor and the charged head groups is not a dominant influence on the electron transfer kinetics.

Electron transport experiments and theory for topologically complex and inhomogeneous structures are fundamentally interesting and may be useful if the structure can be used to modify electron transfer, particularly geminate recombination following forward photoinduced transfer. Experiments are currently in progress to measure electron transfer in micelles and other complex structures on much faster time scales (100 fs) and to obtained detailed information on the influence of topology on geminate recombination.

Acknowledgements

This work was supported by DOE (DE-FG03-84ER13251). The authors thank Hu Cang for his help in setting up the time correlated single photon counting experiment.

References

[1] R.A. Marcus, J. Chem. Phys. 24 (1956) 966.
[2] R.A. Marcus, N. Sutin, Biochim. Biophys. Acta 811 (1985) 265.
[3] J. Jortner, M. Bixon (Eds.), Electron Transfer-from Isolated Molecules to Biomolecules, Wiley, New York, 1999.
[4] M.A. Fox, in: J. Mattay (Ed.), Topics in Current Chemistry, Springer, Berlin, 1991, p. 67.
[5] L. Hammarström, H. Berglund, M. Almgren, J. Phys. Chem. 98 (1994) 9588.
[6] B. Lerebours, Y. Chevalier, M.P. Pileni, Chem. Phys. Lett. 117 (1985) 89.
[7] H.L. Tavernier, A.V. Barzykin, M. Tachiya, M.D. Fayer, J. Phys. Chem. B 102 (1998) 6078.
[8] L. Hammarström, T. Norrby, G. Stenhagen, J. Martensson, B. Akermark, M. Almgren, J. Phys. Chem. B 101 (1997) 7494.
[9] H.L. Tavernier, M.D. Fayer, J. Phys. Chem. B 104 (2000) 11541.
[10] Y.P. Liu, M.D. Newton, J. Phys. Chem. 98 (1994) 7162.
[11] N. Sutin, in: J.R. Bolton, N. Mataga, G. McLendon (Eds.), Electron Transfer in Inorganic, Organic, and Biological Systems, ACS, Washington, 1991, p. 25.
[12] M.R. Wasielewski, in: M.A. Fox, M. Chanon (Eds.), Photoinduced Electron Transfer. Part A: Conceptual Basis, Elsevier, New York, 1988, p. 161.
[13] H. Aota, S. Araki, Y. Morishima, M. Kamachi, Macromolecules 30 (1997) 4090.
[14] C.D. Borsarelli, J.J. Cosa, C.M. Previtali, Photochem. Photobiol. 68 (1998) 438.
[15] J.W.I. Hackett, C. Turro, J. Phys. Chem. A 102 (1998) 5728.
[16] Y. Morishima, H. Aota, K. Saegusa, M. Kamachi, Macromolecules 29 (1996) 6505.
[17] H.L. Tavernier, F. Laine, M.D. Fayer, J. Phys. Chem. A 105 (2001) 8944.
[18] N.M. van Os, J.R. Haak, L.A.M. Rupert, Physico-Chemical Properties of Selected Anionic, Cationic, and Nonionic Surfactants, Elsevier, Amsterdam; New York, 1993.
[19] J.C. Eriksson, G. Gillberg, Acta. Chem. Scand. 20 (1966) 2019.
[20] D.V. O'Conner, D. Philips, Time-Correlated Single Photon Counting, Academic Press, London, 1984.
[21] K. Weidemaier, M.D. Fayer, J. Chem. Phys. 102 (1995) 3820.
[22] K. Weidemaier, M.D. Fayer, J. Phys. Chem. 100 (1996) 3767.
[23] K. Weidemaier, H.L. Tavernier, K.T. Chu, M.D. Fayer, Chem. Phys. Lett. 276 (1997) 309.
[24] K. Weidemaier, H.L. Tavernier, M.D. Fayer, J. Phys. Chem. B 101 (1997) 9352.
[25] J.R. Bolton, M.D. Archer, in: J.R. Bolton, N. Mataga, G. McLendon (Eds.), Electron Transfer in Inorganic, Organic, and Biological Systems, 1991.
[26] R.A. Marcus, J. Chem. Phys. 24 (1956) 979.
[27] D. Rehm, A. Weller, Isr. J. Chem. 8 (1970) 259.
[28] R.A. Marcus, Ann. Rev. Phys. Chem. 15 (1964) 155.
[29] R.A. Marcus, in: P.A. Rock (Ed.), Special Topics in Electrochemistry, Elsevier, Amsterdam, 1977, p. 161.
[30] G.J. Throop, R.J. Bearman, J. Chem. Phys. 42 (1965) 2408.
[31] S.A. Rice, Diffusion-Limited Reactions, Elsevier, Amsterdam, 1985.
[32] S.H. Northrup, J.T. Hynes, J. Chem. Phys. 71 (1979) 871.
[33] K. Weidemaier, H.L. Tavernier, S.F. Swallen, M.D. Fayer, J. Phys. Chem. A 101 (1997) 1887.
[34] H.L. Tavernier, M.M. Kalashnikov, M.D. Fayer, J. Chem. Phys. 113 (2000) 10191.
[35] J.M. Deutch, B.U. Felderhof, J. Chem. Phys. 59 (1973) 1669.
[36] R. Zwanzig, Adv. Chem. Phys. 15 (1969) 325.
[37] H.B. Gray, J.R. Winkler, Annu. Rev. Biochem. 65 (1996) 537.
[38] G.L. Closs, J.R. Miller, Science 240 (1988) 440.
[39] J.R. Miller, J.V. Beitz, R.K. Huddleston, J. Am. Chem. Soc. 106 (1984) 5057.
[40] T. Guarr, G. McLendon, Coordination Chem. Rev. 68 (1985) 1.
[41] R. Itri, L.Q. Amrai, J. Phys. Chem. 95 (1991) 423.
[42] S. Berr, R.R.M. Jones, J.S. Johnson, J. Phys. Chem. 96 (1992) 5611.